

# USP25 promotes hepatocellular carcinoma progression by interacting with TRIM21 via the Wnt/ $\beta$ -catenin signaling pathway

Yinghui Liu<sup>1,2</sup>, Jingjing Ma<sup>3</sup>, Shimin Lu<sup>4</sup>, Pengzhan He<sup>1,2</sup>, Weiguo Dong<sup>1</sup>

<sup>1</sup>Department of Gastroenterology, Renmin Hospital of Wuhan University, Wuhan, Hubei 430060, China;

<sup>2</sup>Central Laboratory of Renmin Hospital, Wuhan, Hubei 430060, China;

<sup>3</sup>Department of Geriatric, Renmin Hospital of Wuhan University, Wuhan, Hubei 430060, China;

<sup>4</sup>Department of Pathology, Renmin Hospital of Wuhan University, Wuhan, Hubei 430060, China.

## Abstract

**Background:** Hepatocellular carcinoma (HCC) is one of the most common malignant tumors in the world. The ubiquitin-specific peptidase 25 (USP25) protein has been reported to participate in the development of several cancers. However, few studies have reported its association with HCC. In this study, we aimed to investigate the function and mechanism of USP25 in the progression of HCC.

**Methods:** We analyzed USP25 protein expression in HCC based on The Cancer Genome Atlas (TCGA) and International Cancer Genome Consortium (ICGC) database cohorts. Then, we constructed USP25-overexpressing and USP25-knockdown HepG2, MHCC97H, and L-O2 cells. We detected the biological function of USP25 by performing a series of assays, such as Cell Counting Kit-8 (CCK-8), colony formation, transwell, and wound healing assays. Western blotting and quantitative real-time polymerase chain reaction (qRT-PCR) analyses were performed to detect the interaction between USP25 and the Wnt/ $\beta$ -catenin signaling pathway. The relationship between USP25 and tripartite motif-containing 21 (TRIM21) was assessed through mass spectrometry and co-immunoprecipitation (Co-IP) analysis. Finally, we constructed a mouse liver cancer model with the USP25 gene deletion to verify *in vivo* role of USP25.

**Results:** USP25 was highly expressed in HCC tissue and HCC cell lines. Importantly, high expression of USP25 in tissues was closely related to a poor prognosis. USP25 knockdown markedly reduced the proliferation, migration, and invasion of HepG2 and MHCC97H cells, whereas USP25 overexpression led to the opposite effects. In addition, we demonstrated that USP25 interacts with TRIM21 to regulate the expression of proteins related to epithelial–mesenchymal transition (EMT; E-cadherin, N-cadherin, and Snail) and the Wnt/ $\beta$ -catenin pathway ( $\beta$ -catenin, Adenomatous polyposis coli, Axin2 and Glycogen synthase kinase 3 beta) and those of their downstream proteins (C-myc and Cyclin D1). Finally, we verified that knocking out USP25 inhibited tumor growth and distant metastasis *in vivo*.

**Conclusions:** In summary, our data showed that USP25 was overexpressed in HCC. USP25 promoted the proliferation, migration, invasion, and EMT of HCC cells by interacting with TRIM21 to activate the  $\beta$ -catenin signaling pathway.

**Keywords:** Hepatocellular carcinomas; USP25 protein, human; TRIM21 protein, human; Wnt/ $\beta$ -catenin signaling pathway; Epithelial–mesenchymal transition

## Introduction

Hepatocellular carcinoma (HCC) is one of the most common malignant tumors worldwide,<sup>[1]</sup> and its incidence and mortality rates have gradually increased in recent years.<sup>[2]</sup> The current treatment for HCC is mainly comprehensive therapy based on surgical resection; however, owing to the high recurrence and metastasis rates, the 5-year survival rate is only 19%, which indicates its profound effect on patient quality of life.<sup>[3]</sup> Therefore, studying the mechanisms regulating HCC cell invasion and migration and identifying novel biomarkers are vital for the diagnosis and treatment of HCC.

Deubiquitinating enzymes (DUBs) play crucial roles in regulating various signal transduction pathways and biological processes, such as apoptosis, cell proliferation, and DNA repair.<sup>[4–6]</sup> Ubiquitin-specific peptidase 25 (USP25) is a DUB gene located on chromosome 21q11.2, which is a region with one of the lowest gene densities in the human genome, and is expressed at high levels in the embryonic mouse brain and testis.<sup>[7]</sup> As previously reported, USP25 participates in the development of colon, lung, breast, and prostate cancer and is expected to be a target for tumor therapy.<sup>[8]</sup> A study showed that USP25 interacts with Tankyrase 1 (TNKS1)

Yinghui Liu, Jingjing Ma, and Shimin Lu contributed equally to this work.

**Correspondence to:** Dr. Weiguo Dong, Department of Gastroenterology, Renmin Hospital of Wuhan University, Wuhan, Hubei 430060, China  
E-Mail: dongweiguo@whu.edu.cn

Copyright © 2023 The Chinese Medical Association, produced by Wolters Kluwer, Inc. under the CC-BY-NC-ND license. This is an open access article distributed under the terms of the Creative Commons Attribution-Non Commercial-No Derivatives License 4.0 (CCBY-NC-ND), where it is permissible to download and share the work provided it is properly cited. The work cannot be changed in any way or used commercially without permission from the journal.

Chinese Medical Journal 2023;136(18)

**Received:** 26-12-2022; **Online:** 13-07-2023 **Edited by:** Jinjiao Li and Yuanyuan Ji

Access this article online

Quick Response Code:



Website:  
www.cmj.org

DOI:  
10.1097/CM9.0000000000002714

to positively regulate the Wnt/ $\beta$ -catenin signaling pathway.<sup>[9]</sup> The Wnt/ $\beta$ -catenin signaling pathway, known as the canonical Wnt signaling pathway, is a highly conserved developmental signal transduction pathway.<sup>[10]</sup> In the process of embryonic development and tissue homeostasis, the canonical Wnt signaling pathway regulates cell proliferation, differentiation, polarity, and apoptosis. Abnormal activation of the Wnt/ $\beta$ -catenin signaling pathway is involved in tumor development.<sup>[11]</sup>

In our study, we investigated the function and mechanism of USP25, which is involved in the progression of HCC.

## Methods

### Expression of USP25 as determined by bioinformatics analysis

The Cancer Genome Atlas-Liver Hepatocellular Carcinoma (TCGA-LIHC) dataset contains data on 371 HCC patients undergoing tertiary RNA sequencing (RNA-seq). In addition, data from another 240 tumor samples and 202 adjacent tissues were obtained from the International Cancer Genome Consortium (ICGC) web portal (<https://dcc.icgc.org/projects/LIRI-JP>). The data in both the TCGA and ICGC databases are publicly available. In this study, we followed the data access policy and publication guidelines of the TCGA and ICGC. The Tumor Immune Estimation Resources (TIMER v2.0; <https://cistrome.shinyapps.io/timer/>) and The University of Alabama at Birmingham CANcer data analysis Portal (UALCAN; <http://ualcan.path.uab.edu/index.html>) are unified databases that can be used to analyze the mRNA levels of different tumor types based on TCGA data. The correlation between USP25 gene expression and the prognosis of 370 HCC patients was explored by using the Kaplan–Meier plotter database (<https://kmplot.com/analysis/>).

### Cell lines and cell culture

Six human HCC cell lines (HepG2, HuH7, SMMC7721, Bel7402, MHCC97H, and PLC/PRF/5) and a normal hepatocyte cell line (L-O2) were obtained from the China Center for Type Culture Collection (Wuhan, China). The cell lines were cultured in Dulbecco's modified Eagle medium (DMEM, HyClone, Thermo Fisher Scientific, USA) supplemented with 10% fetal bovine serum (FBS; Gibco, USA) and a 1% antibiotic solution (100 U/mL penicillin and 100 g/mL streptomycin; Beyotime, China) at 37°C in a humidified incubator with 5% CO<sub>2</sub>.

### Transfection of lentiviral plasmids

Lentiviruses were constructed and purchased from GeneChem (Shanghai, China) [Supplementary Figure 1, <http://links.lww.com/CM9/B575>]. Then, only the L-O2, HepG2, and MHCC97H cells were infected according to the established protocol and selected with puromycin to obtain stable USP25-transfected cell lines. Transient transfection was performed with a TRIM21 (tripartite motif-containing 21) overexpression plasmid (GeneChem) and

Lipofectamine 2000 transfection reagent (Thermo Fisher, Waltham, MA, USA) [Supplementary Figure 2A, <http://links.lww.com/CM9/B575>].

### Quantitative real-time polymerase chain reaction (qRT-PCR)

Total RNA was extracted by utilizing a TRIzol kit (Omega, Norcross, GA, USA) and subjected to reverse transcription. Real-time PCR was performed with the SYBR green protocol using gene-specific primers [Supplementary Table 1, <http://links.lww.com/CM9/B575>]. The levels of the target mRNAs were normalized to those of  $\beta$ -actin to calculate the relative mRNA expression.

### Western blotting

The stably transfected cell lines were pretreated with 10  $\mu$ mol/L XAV939 (Selleck, China) for 24 h [Supplementary Figure 2A, <http://links.lww.com/CM9/B575>]. Nuclear and cytoplasmic protein extraction kits were used to extract nuclear and cytoplasmic proteins in HCC cells, respectively (Beyotime). Total cell protein was extracted with radioimmunoprecipitation assay (RIPA) buffer supplemented with phenylmethylsulfonyl fluoride (PMSF) and protease inhibitors (Beyotime). A Bicinchoninic acid (BCA) protein assay kit (Beyotime) was used to measure protein concentrations according to the manufacturer's instructions. The proteins were separated by 10% sodium dodecyl sulfate-polyacrylamide gel electrophoresis (SDS-PAGE) and transferred to polyvinylidene difluoride (PVDF) membranes (Millipore, USA) with a wet transfer system. Then, the membranes were blocked with 5% non-fat milk in tris buffered saline tween (TBST) for 1 h and incubated with several primary antibodies overnight at 4°C and with secondary antibodies for 1 h at room temperature. We purchased the antibodies against the following proteins: USP25 (1:1000) (Abcam, USA), GAPDH (Glyceraldehyde-3-phosphate dehydrogenase, 1:1000; Cell Signaling Technology, USA), PCNA (Proliferating Cell Nuclear Antigen, 1:20000; Proteintech, China), MMP2 (Matrix metalloproteinase 2, 1:1000; Cell Signaling Technology), MMP9 (Matrix metalloproteinase 9, 1:1000; Cell Signaling Technology), N-cadherin (1:2000; Proteintech), E-cadherin (1:1000; Cell Signaling Technology), Snail (1:1000; Cell Signaling Technology), Vimentin (1:5000; Proteintech), Axin2 (1:1000; Proteintech),  $\beta$ -catenin (1:5000; Proteintech), C-myc (1:2000; Proteintech), Cyclin D1 (1:5000; Proteintech), Glycogen synthase kinase 3 beta (GSK3 $\beta$ ; 1:1000; Proteintech), and TRIM21 (1:1000; Proteintech). Finally, enhanced chemiluminescence (ECL) reagent (Biosharp, China) was used for Western blotting, and the protein expression values were determined with an ECL system (Bio-Rad, USA).

### Cell proliferation analyses

#### Colony formation assay

Three thousand cells per well were seeded in a 6-well plate. Two weeks later, the cells were fixed in 4% paraformaldehyde and stained with 0.5% crystal violet.

### Cell counting kit-8 (CCK-8)

Cells were separately seeded into 96-well plates and cultured for 24 h, 48 h, and 72 h. Then, 10  $\mu$ L of CCK-8 (Beyotime) solution was added to each well, and the cells were incubated for an additional 2 h. Ultimately, the optical density was estimated by measuring the absorbance of the colored formazan reaction product at 450 nm with a microplate reader (Victor3 1420 Multi-label Counter, Perkin Elmer).

### EdU analysis

The DNA synthesis rate was measured with a 5-ethyl-20-deoxyuridine (EdU) assay kit (BeyoClick™ EdU-594, Beyotime). After incubation in EdU for 2 h and fixation with 4% paraformaldehyde, the cells were lysed in 0.1% Triton X-100 for 10 min, incubated with 3% bovine serum albumin (BSA) for 15 min, and finally incubated with a fluorescently labeled additive in solution for 30 min.

### Cell migration and invasion assays

Cells were digested, and a total of 100  $\mu$ L of the cell suspension was seeded in the upper chamber of a Transwell insert (CORNING, USA) with 8- $\mu$ m pores. The inserts were precoated with Matrigel (BD Biosciences, USA) for the invasion assay, but the inserts used for the migration assay were uncoated. The lower chamber was filled with 600  $\mu$ L of medium supplemented with 25% FBS. Twenty-four hours later, the inserts were fixed with a 4% paraformaldehyde solution for 15 min and stained with 0.1% crystal violet for 30 min. The cells were observed and counted in eight random fields under a microscope.

Cells were cultured in a 6-well plate until the cells reached 100% confluence, and then, two vertical lines were scratched across the monolayer with the tip of a 100- $\mu$ L sterile pipette. Then, the serum-free medium was replaced with fresh medium, and the wound was observed and photographed at 0 h and 48 h under a microscope.

### Immunofluorescence (IF) analysis

Cells were seeded onto glass coverslips in a 24-well plate for 24 h. Then, the cells were fixed with 4% paraformaldehyde for 15 min, permeabilized with 0.1% Triton X-100, and blocked with 3% BSA. Next, the cells on the coverslips were further incubated overnight at 4°C with a specific primary antibody. The next day, the cells were incubated with fluorescently labeled secondary antibodies for 1 h at room temperature in the dark. The nuclei were stained with 4',6-diamidino-2'-phenylindole (DAPI; Beyotime). The cells were observed using an upright fluorescence microscope (BX51, Olympus, Japan) and a confocal fluorescence microscope (BX63, Olympus Optical Ltd., Tokyo, Japan).

### Co-immunoprecipitation (Co-IP) analysis

We added immunoprecipitation lysate NP40 (Biosharp) to the cells and extracted the total protein after cell lysis on ice for 30 min. After preclearance by adding 10  $\mu$ L of

protein A/G agarose (Pierce, Dallas, TX, USA) to the cell lysate, the supernatant was incubated with 20  $\mu$ L of protein A/G agarose and anti-FLAG or anti-hemagglutinin (HA) tag antibody at 4°C overnight. After the precipitates were washed five times with phosphate buffered saline (PBS), 5 $\times$  loading buffer was added, and the results were analyzed by Western blotting.

### Immunohistochemistry (IHC)

Liver tissue sections were deparaffinized and rehydrated in graded ethanol solutions and then boiled in 10 mmol/L citrate buffer (pH 6.0) in a pressure cooker for antigen retrieval. Finally, the tissue sections were incubated with specific antibodies (1: 200 dilution). The sections were stained with 3,3'-diaminobenzidine (DAB) and hematoxylin.

### Hematoxylin and eosin (HE) staining and reticular fiber staining

For HE and reticular fiber staining, extracted tissues were fixed, dehydrated with an ethanol gradient, and embedded in paraffin. Mouse liver and lung tissues were cut into 4- $\mu$ m-thick sections and stained with HE and reticular fiber staining solution. The specimens were observed with an upright fluorescence microscope.

### In vivo mouse model

Wild-type (WT) and C57BL/6 (USP25<sup>-/-</sup>) mice were bred in house in a specific-pathogen-free (SPF) environment with free access to food and water and a 12-h dark/light cycle. The newborn male mice of WT and USP25<sup>-/-</sup> mice were randomly divided into two groups such as model and control groups respectively, with seven mice in each group. Male mice were intraperitoneally injected with N-diethylnitrosamine (Sigma, USA) 2 weeks after birth at a concentration of 25 mg/kg body weight or with an equal amount of PBS solution. Then we obtained four groups: the USP25<sup>-/-</sup>/DEN, WT/DEN, USP25<sup>-/-</sup>/PBS, and WT/PBS groups. The mice were weighed 30 weeks after injection, and mouse livers were harvested to analyze tumor formation [Supplementary Figure 2B, <http://links.lww.com/CM9/B575>]. This study was approved by the Institutional Animal Care and Use Committee of the Renmin Hospital of Wuhan University (No. WDRM20190316, Supplementary Figure 3, <http://links.lww.com/CM9/B575>).

### Statistical analysis

The data were analyzed by SPSS 23.0 (IBM Information Management, USA) software for Microsoft Windows and are expressed as the mean  $\pm$  standard deviation (SD). The significance of differences among groups was determined by analysis of variance (ANOVA). A value of  $P < 0.05$  was considered to indicate statistical significance.

## Results

### USP25 is highly expressed in HCC and correlated with a poor prognosis

To determine the expression of USP25 in HCC, we studied the expression of USP25 across cancers and found that it was differentially expressed between tumor

and peritumor tissues and was particularly highly expressed in liver cancer [Figure 1A]. In addition, we analyzed mRNA datasets in the TCGA and ICGC databases, and the results similarly showed that the expression of USP25 was higher in liver tumor tissues than in peritumor tissues [Figure 1B]. For further validation, we performed Western blotting of the proteins in HCC and normal cell lines, and we observed that the expression level of USP25 was significantly higher in the six HCC cell lines (HepG2, HuH7, SMMC7721, Bel7402, MHCC97H, and PLC/PRF/5) than in the normal hepatocyte cell line (L-O2) [Figure 1C]. In addition, the expression level of USP25 in HCC cells in the Cancer Cell Line Encyclopedia (CCLE) database was determined to verify the Western blotting results [Figure 1D]. Moreover, a survival analysis showed that high USP25 expression was significantly correlated with poor overall survival [Figure 1E]. We also observed that the higher the tumor malignancy degree of HCC patients was, the lower the methylation level of the USP25 promoter was *in vivo* [Figure 1F] and that the higher the expression of USP25 was, the higher the number of nodal metastases was [Figure 1G]. In summary, these observations verified that USP25 may contribute to the development of liver cancer.

#### **USP25 promotes HCC cell proliferation, migration, and invasion *in vitro***

We confirmed that USP25 was highly expressed in HCC; therefore, to further explore the biological function of USP25, we first constructed HCC cell lines with USP25 overexpression or knockdown called “HepG2/MHCC97H-USP25” and “HepG2/MHCC97H-shUSP25” cells, respectively [Figure 2A–C]. We also constructed normal cell lines called “L-O2-USP25” and “L-O2-shUSP25” [Supplementary Figure 4A, B, <http://links.lww.com/CM9/B575>]. Then, we performed a series of assays to determine whether USP25 regulates tumor cell proliferation and metastasis. The results of a colony formation assay revealed that knocking down USP25 expression inhibited the colony formation of HepG2 and MHCC97H cells compared with that in the control group cells [Figure 2D, E]. Moreover, the CCK-8 assay indicated that USP25 depletion dramatically decreased the proliferation of HepG2 and MHCC97H cells [Figure 2F]. EdU incorporation into newly synthesized DNA strands allows visualization of red fluorescence via fluorescence microscopy. Compared with the control cell group, the HepG2/MHCC97H-USP25 group showed more EdU-positive cells, and cell proliferation was remarkably inhibited in the HepG2/MHCC97H-shUSP25 group [Figure 2G–J]. The results of a series of assays revealed that there was no significant difference between the control, L-O2-shUSP25, vector, and L-O2-USP25 groups [Supplementary Figure 4C–G, <http://links.lww.com/CM9/B575>]. The proliferation capacity was not significantly different between L-O2-shUSP25 and HepG2/MHCC97H-shUSP25 cells, while the proliferation capacity was significantly increased in HepG2 and MHCC97H cells with USP25 overexpression compared to L-O2 cells with USP25 overexpression [Supplementary Figure 4H,

<http://links.lww.com/CM9/B575>]. Furthermore, migration and invasion assays were performed, and the results revealed that USP25 overexpression increased the migratory and invasive capacities of HepG2 and MHCC97H cells, whereas knocking down USP25 expression had the opposite effects on these cells [Figure 3A–D]. Moreover, a wound healing test showed that the relative scratch width was reduced significantly in the HepG2/MHCC97H-USP25 group, indicating that the cell migratory ability was high in this group [Figure 3E–H]. Finally, Western blotting was performed to detect the expression levels of a proliferation-related protein (PCNA) and invasion-related proteins (MMP2 and MMP9). The results indicated that in both HepG2 and MHCC97H cells, these protein expression levels were all significantly higher in the USP25 overexpression group than in the empty vector (vector) group, while knocking down USP25 expression in these cells induced the opposite effects [Figure 3I, J]. Collectively, these results demonstrated that USP25 promotes HCC cell proliferation, migration, and invasion.

#### **USP25 regulates cancer progression via the EMT in HCC cells**

EMT has been proposed to be a critical mechanism involved in cancer progression and metastasis; therefore, we examined whether USP25 expression was correlated with EMT in HCC. Cell IF staining and Western blotting were performed to explore the expression of indicators associated with EMT. The results of the IF assays showed that N-cadherin and E-cadherin were mainly expressed on the cell membrane, while USP25 was expressed in the cytoplasm [Figure 4A, B]. The results of Western blotting led to similar conclusions, and we observed that the N-cadherin, Vimentin, and Snail protein expression levels increased while the E-cadherin protein expression was markedly decreased in the HepG2-USP25 group [Figure 4C]. However, the opposite result was observed in the MHCC97H-shUSP25 group [Figure 4D]. In summary, we validated that USP25 can regulate EMT to promote HCC progression.

#### **USP25 promotes HCC growth by activating the Wnt/ $\beta$ -catenin signaling pathway**

To further clarify the underlying mechanism by which USP25 regulates HCC, we surveyed the relevant literature and found that the Wnt/ $\beta$ -catenin signaling pathway plays a significant role in HCC development. The IF results revealed clear changes in  $\beta$ -catenin expression between the HepG2-USP25 and MHCC97H-shUSP25 groups and demonstrated that  $\beta$ -catenin was mainly localized in the cell nucleus [Figure 5A]. According to the results of Western blotting of nuclear-cytoplasmic fractions, the expression level of  $\beta$ -catenin increased both in the cytoplasm and nucleus in the HepG2-USP25 group *vs.* the corresponding control group, while the results showed the opposite trends in the MHCC97H-shUSP25 group *vs.* the corresponding control group [Figure 5B]. Subsequently, we detected the signaling pathway and the mRNA and protein expression levels of its downstream factors by performing qRT-PCR and Western blotting analyses. We found that the mRNA expression level of the Wnt/ $\beta$ -catenin pathway-related

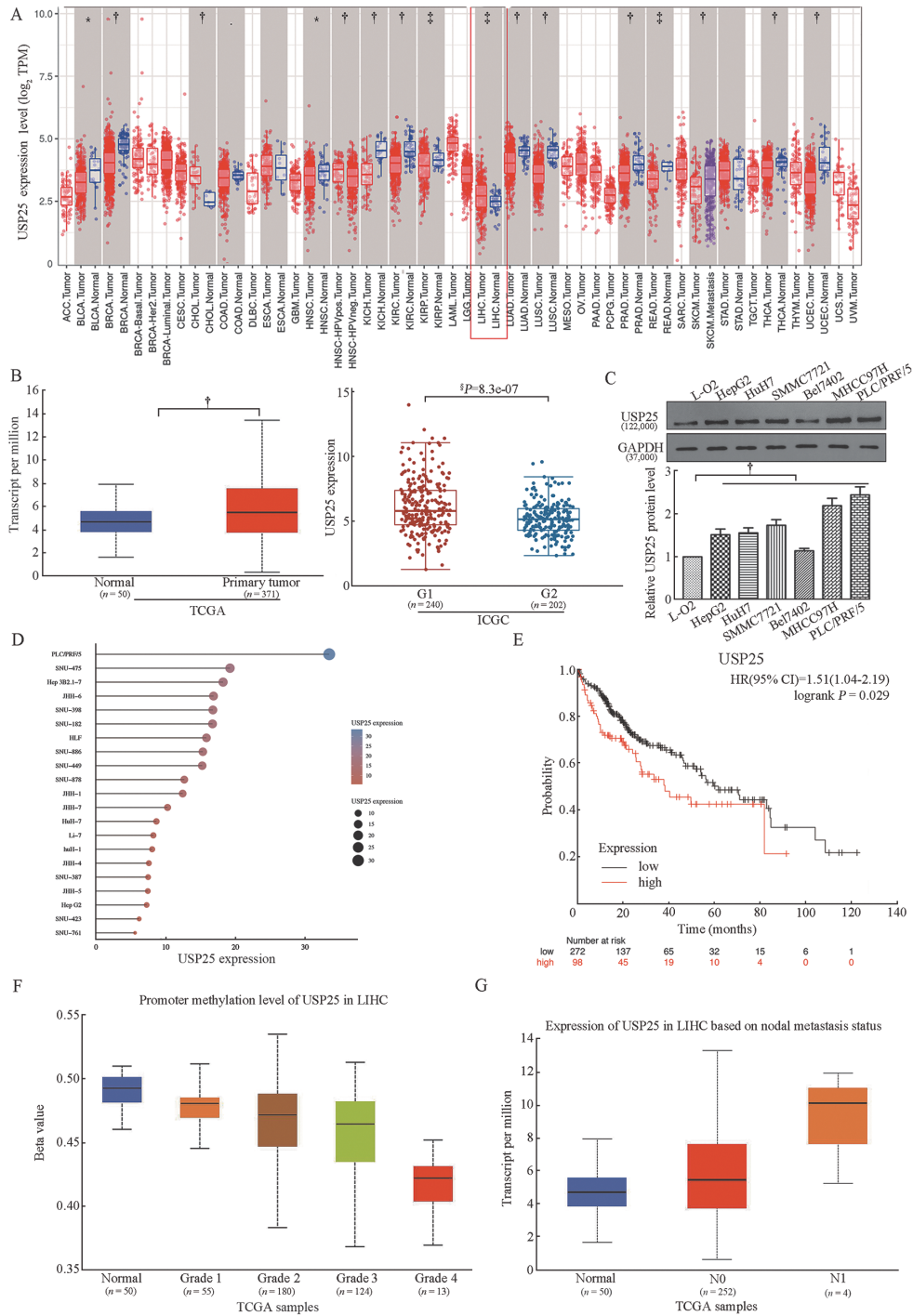


**Figure 1:** USP25 is highly expressed in HCC and is correlated with poor prognosis. (A) The expression of USP25 in pan-carcinoma as determined with the TIMER database. (B) The expression of USP25 mRNA was analyzed in HCC tissues from TCGA and ICGC databases. (C) The protein expression levels of USP25 in a normal liver cell line and six HCC cell lines. (D) The expression of USP25 in different HCC cell lines in the CCLE database. (E) Kaplan–Meier survival analysis of survival in HCC patients grouped according to USP25 expression ( $n = 370$ ). (F) The promoter methylation level of USP25 in different grades of HCC according to the analysis of patient samples. Grade 1: well differentiated; Grade 2: moderately-differentiated; Grade 3: moderately and poorly differentiated; Grade 4: poorly differentiated. (G) The expression of USP25 in HCC patients based on nodal metastasis status. \* $P < 0.05$ ; † $P < 0.001$ ; ‡ $P < 0.01$ ; § $P < 0.0001$ . ACC: Adrenocortical carcinoma; BLCA: Bladder urothelial carcinoma; BRCA: Breast invasive carcinoma; CESC: Cervical squamous cell carcinoma; CHOL: Cholangiocarcinoma; COAD: Colon adenocarcinoma; DLBC: Lymphoid neoplasm diffuse large B-cell lymphoma; ESCA: Esophageal carcinoma; GBM: Glioblastoma multiforme; HNSC: head and neck squamous cell carcinoma; KICH: Kidney chromophobe; KIRC: Kidney renal clear cell carcinoma; KIRP: Kidney renal papillary cell carcinoma; LAML: Acute myeloid leukemia; LGG: Brain lower grade glioma; LIHC: Liver hepatocellular carcinoma; LUAD: Lung adenocarcinoma; LUSC: Lung squamous cell carcinoma; MESO: Mesothelioma; OV: Ovarian serous cystadenocarcinoma; PAAD: Pancreatic adenocarcinoma; PCPG: Pheochromocytoma and paraganglioma; PRAD: Prostate adenocarcinoma; READ: Rectum adenocarcinoma; SARC: Sarcoma; SKCM: Skin cutaneous melanoma; STAD: Stomach adenocarcinoma; TGCT: Testicular germ cell tumors; THCA: Thyroid carcinoma; THYM: Thymoma; UCS: Uterine corpus endometrial carcinoma; UCS: Uterine carcinosarcoma; UVM: Uveal melanoma; HCC: Hepatocellular carcinoma; ICGC: International Cancer Genome Consortium; TIMER: Tumor Immune Estimation Resource; USP25: Ubiquitin-specific peptidase 25; TCGA: The Cancer Genome Atlas; CCLE: Cancer Cell Line Encyclopedia; HR: Hazard ratio; L-02: Normal hepatocyte cell line; GAPDH: Glyceraldehyde-3-phosphate dehydrogenase; N0, 1: Node0,1.

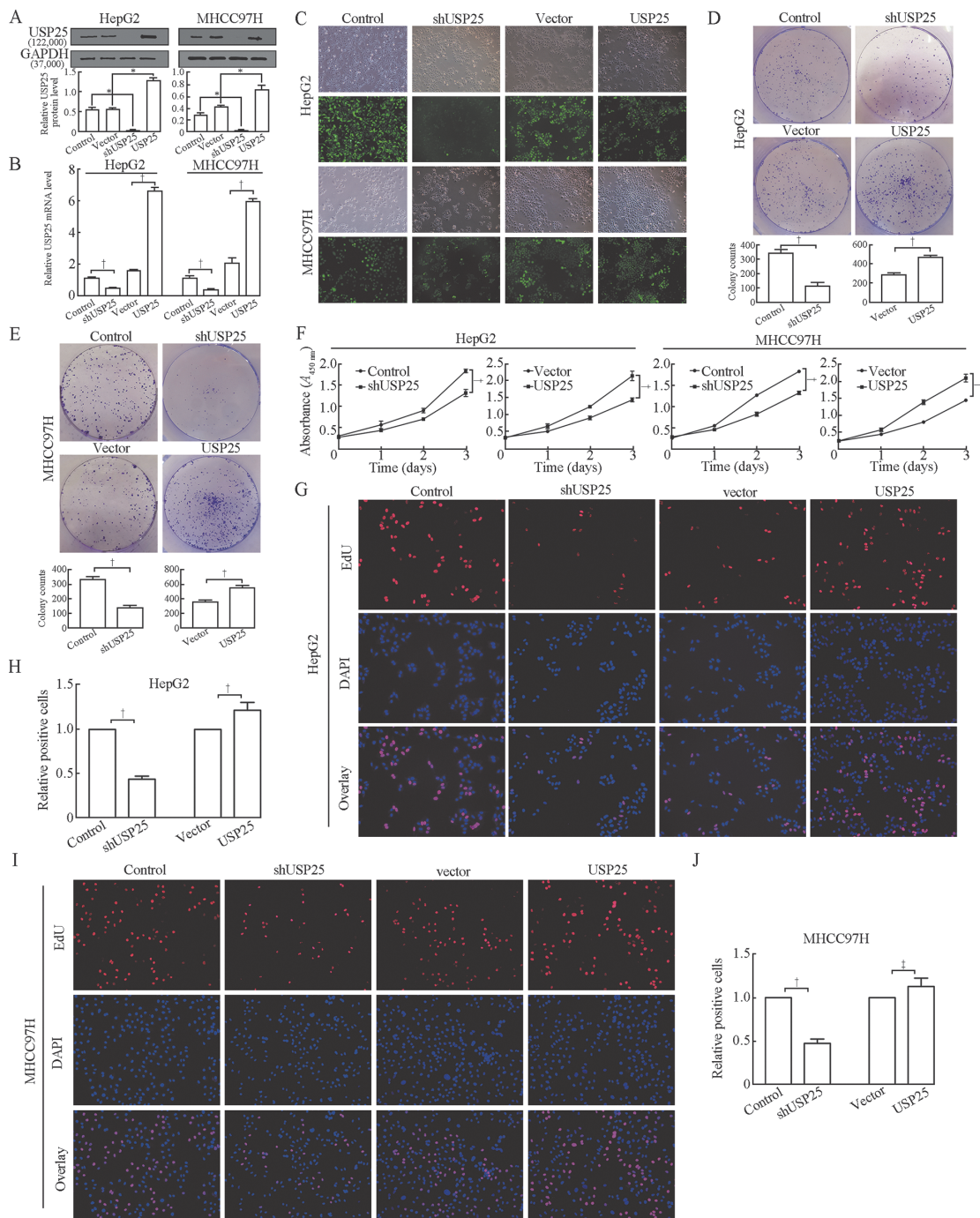


**Figure 2:** USP25 promotes HCC cell proliferation *in vitro*. (A–C) HepG2 and MHCC97H cell lines with USP25 overexpression or knockdown were successfully established, as verified by analysis of protein and mRNA levels and fluorescence microscopy (Original magnification  $\times 100$ ). (D–F) Colony formation and CCK-8 assays were performed to detect cell proliferation. (G–J) DNA synthesis was measured by EdU IF staining (Original magnification  $\times 200$ ). \* $P < 0.05$ ; † $P < 0.001$ ; ‡ $P < 0.01$ . CCK-8: Cell counting kit-8; HCC: Hepatocellular carcinoma; IF: Immunofluorescence; USP25: Ubiquitin-specific peptidase 25; EdU: 5-ethynyl-2-deoxyuridine; DAPI: 4',6-Diamidino-2'-phenylindole; shUSP25: short hairpin Ubiquitin-specific peptidase 25; GAPDH: Glyceraldehyde-3-phosphate dehydrogenase.

factor  $\beta$ -catenin increased, while the expression levels of Axin2, APC, and GSK3 $\beta$  decreased in the HepG2-USP25 group *vs.* the corresponding control group. However, the opposite trends were observed when USP25 expression was knocked down in MHCC97H cells [Figure 5C]. The Western blotting results demonstrated that the expression level of the pathway-related protein  $\beta$ -catenin and the downstream factors C-myc and Cyclin D1 increased

significantly, while those of Axin2 and GSK3 $\beta$  decreased in the HepG2-USP25 group *vs.* the corresponding control group [Figure 5D]. The Western blotting results of the MHCC97H-shUSP25 group showed the opposite trends [Figure 5E]. To determine the relationship between USP25 expression, EMT and Wnt/ $\beta$ -catenin signaling pathway activation, we treated cells with XAV939, a specific tankyrase inhibitor, to inhibit Wnt/ $\beta$ -catenin

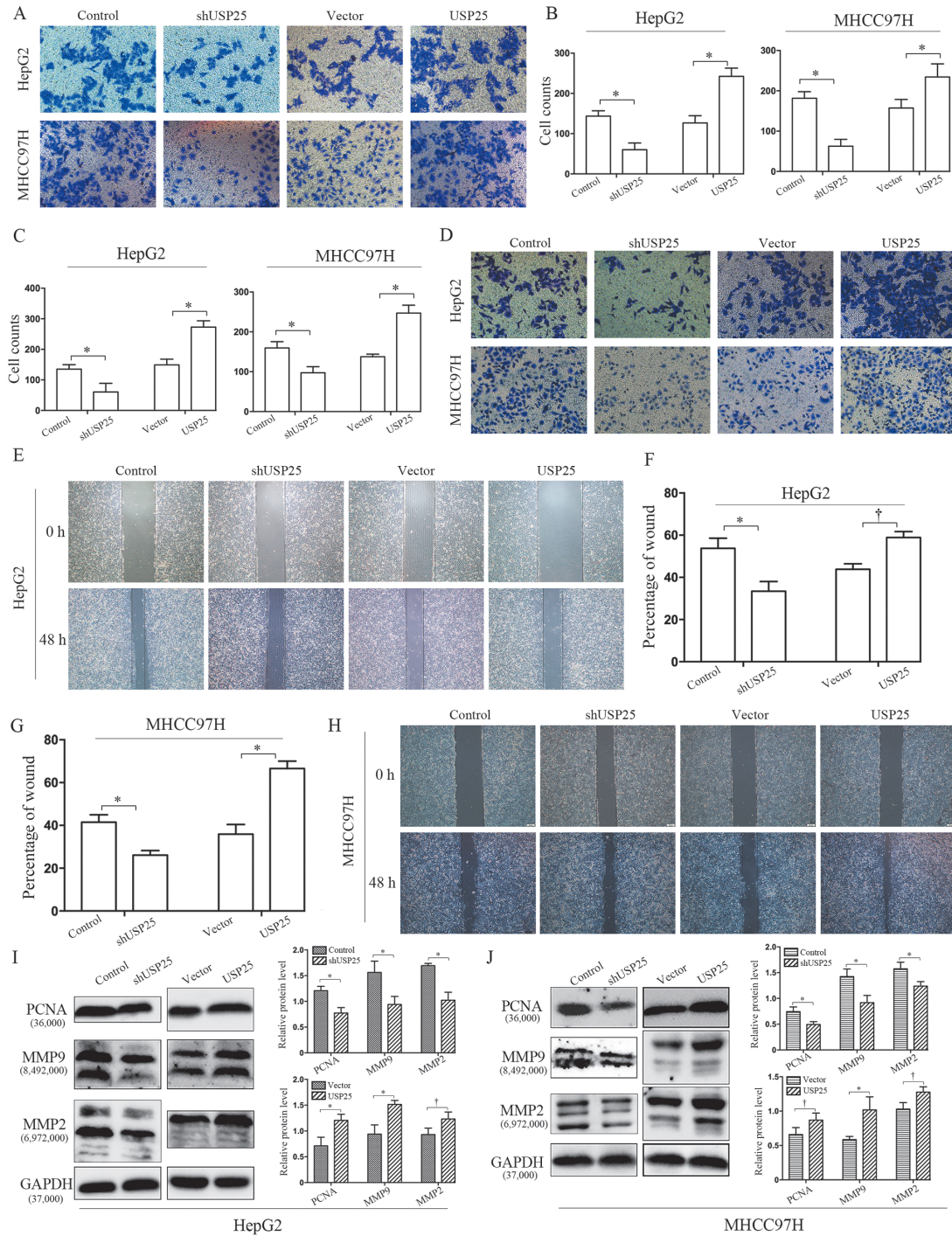


**Figure 3:** USP25 promotes HCC cell migration and invasion *in vitro*. (A,B) A Transwell invasion assay was performed to assess the invasiveness of HepG2 and MHCC97H cells (Original magnification  $\times 100$ ). (C,D) A transwell migration assay was performed to analyze the migratory ability of HepG2 and MHCC97H cells (Original magnification  $\times 100$ ). (E–H) The scratch assay results demonstrated the migratory ability of HepG2 and MHCC97H cells (Original magnification  $\times 40$ ). (I,J) The expression levels of a PCNA and invasion-related proteins (MMP2 and MMP9) were detected by Western blotting. \* $P < 0.001$ ; † $P < 0.01$ . HCC: Hepatocellular carcinoma; PCNA: Proliferation-related protein; USP25: Ubiquitin-specific peptidase 25; MMP2: Matrix metalloproteinase 2; MMP9: Matrix metalloproteinase 9; shUSP25: short hairpin Ubiquitin-specific peptidase 25; GAPDH: Glyceraldehyde-3-phosphate dehydrogenase.

signaling. The pathway inhibitor XAV939 reduced the enhancing effect of USP25 overexpression on HepG2 cells, and the expression of proteins related to EMT changed correspondingly. However, the inhibitor XAV939 did not noticeably alter the levels of these

proteins in the MHCC97H-shUSP25 group [Figure 5F,G]. Thus, we confirmed that USP25 can regulate EMT by activating the Wnt/ $\beta$ -catenin signaling pathway to promote HCC progression.

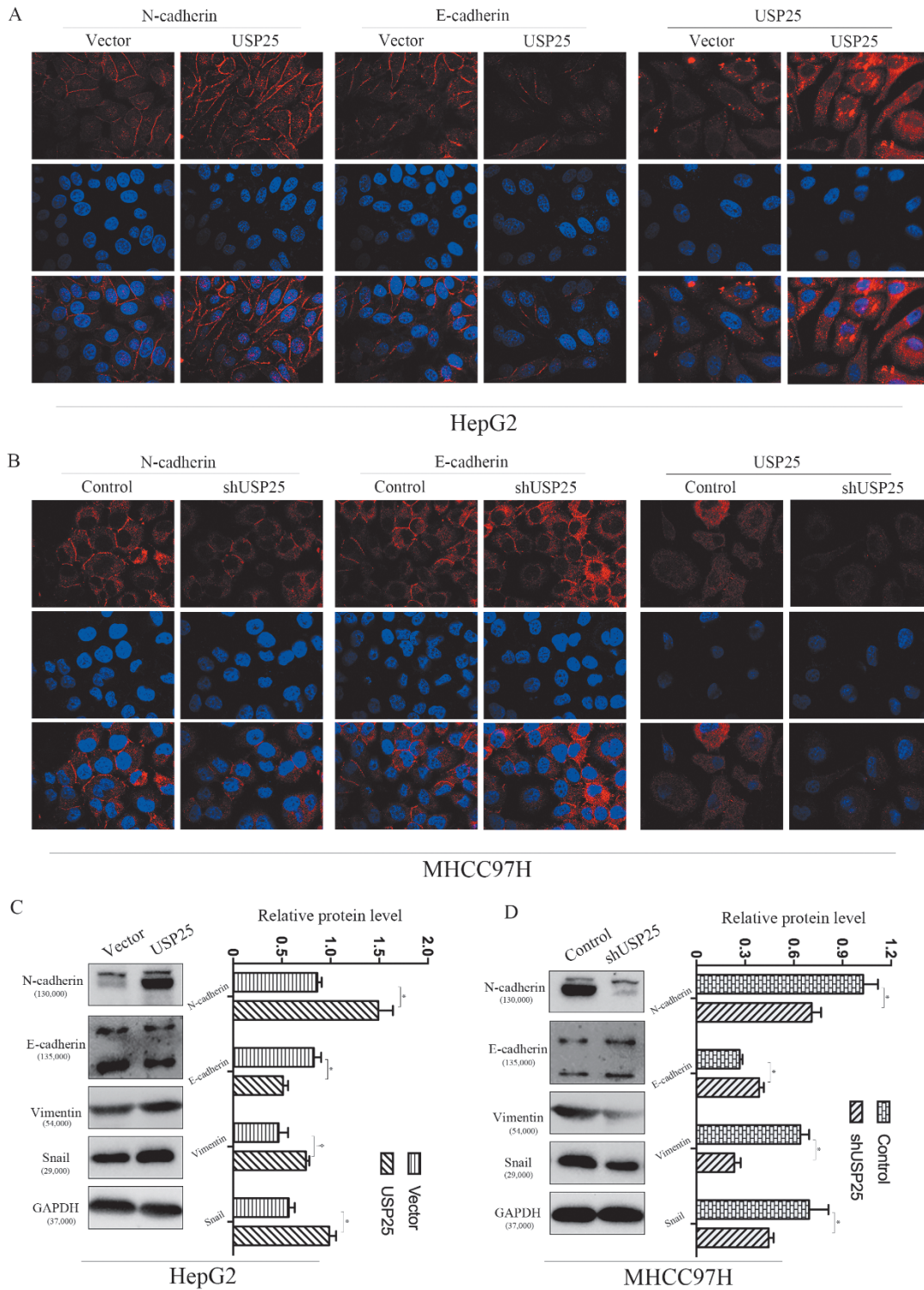


**Figure 4:** USP25 regulates HCC progression via EMT of HCC cells. (A,B) IF staining was performed to detect the expression of USP25 and the related proteins involved in EMT (Original magnification  $\times 1000$ ). (C,D) Western blotting was performed to detect the expression levels of EMT-related proteins. \* $P < 0.001$ ; † $P < 0.01$ . EMT: Epithelial–mesenchymal transition; HCC: Hepatocellular carcinoma; IF: Immunofluorescence; USP25: Ubiquitin-specific peptidase 25; GAPDH: Glyceraldehyde-3-phosphate dehydrogenase; shUSP25: Short hairpin Ubiquitin-specific peptidase 25.



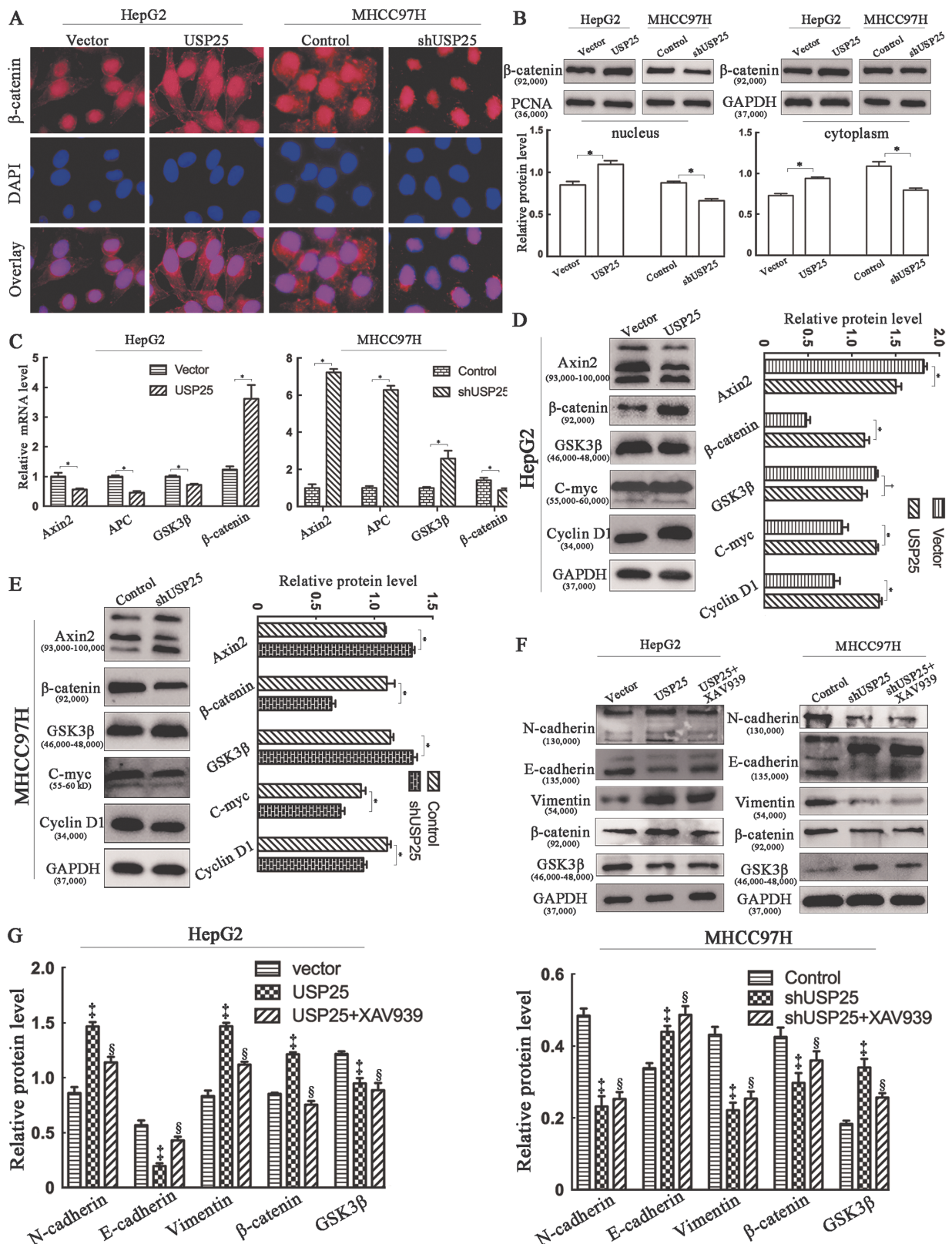


**Figure 5:** USP25 promotes HCC growth by activating the Wnt/ $\beta$ -catenin signaling pathway. (A) The expression of  $\beta$ -catenin was observed by IF staining (Original magnification  $\times 200$ ). (B) The mRNA expression of components in the Wnt/ $\beta$ -catenin signaling pathway was measured by qRT-PCR. (C) The expression of  $\beta$ -catenin was observed by Western blotting of nuclear-cytoplasmic fractionation. (D, E) Western blotting was used to detect the protein expression levels of Wnt/ $\beta$ -catenin pathway components and downstream factors. (F, G) Western blotting analysis after XAV939 treatment of HepG2 and MHCC97H cells. \* $P < 0.001$ ;  $^{\dagger}P < 0.01$ ;  $^{\ddagger}P < 0.05$ , shUSP25 vs. Control;  $^{\S}P < 0.05$ , shUSP25+XAV939 vs. Control. HCC: Hepatocellular carcinoma; IF: Immunofluorescence; qRT-PCR: Quantitative real-time polymerase chain reactio; USP25: Ubiquitin-specific peptidase 25. DAPI: 4',6-Diamidino-2'-phenylindole; shUSP25: Short hairpin Ubiquitin-specific peptidase 25; PCNA: Proliferating cell nuclear antigen GAPDH: Glyceraldehyde-3-phosphate dehydrogenase; GSK3 $\beta$ : Glycogen synthase kinase 3 beta.

### USP25 interacts with TRIM21 to activate the Wnt/ $\beta$ -catenin signaling pathway

To further investigate the molecular mechanisms by which USP25 activates the Wnt/ $\beta$ -catenin signaling pathway, we screened USP25-interacting factors by mass spectrometry. The mass spectrometry results showed 713 differentially expressed proteins (DEPs) [Figure 6A and Supplementary Table 2, <http://links.lww.com/CM9/B575>], and the secondary mass spectrum of USP25 is shown in Figure 6B. Among the differentially regulated proteins, we selected TRIM21 for further study because it had been suggested to participate in HCC progression in previous reports. The results of a molecular docking analysis showed an interaction between USP25 and TRIM21 (ZDOCK [<http://zdock.umassmed.edu/>] Score: 1725) [Figure 6C], and a TCGA database showed that USP25 was positively correlated with TRIM21 by using the Pearson correlation analysis [Figure 6D]. To verify that USP25 interacted with TRIM21 to activate the Wnt/ $\beta$ -catenin signaling pathway, we performed the following experiments: IF staining showed that USP25 and TRIM21 were located in both the cytoplasm and nucleus [Figure 6E]. To characterize the potential cooperative roles of USP25 and TRIM21, we performed Co-IP to test whether the two proteins are involved in a protein-protein interaction [Figure 6F]. In addition, we observed that TRIM21 overexpression in MHCC97H cells rescued cell migratory and invasive capacity, which had been weakened by USP25 knockdown [Figure 6G–J]. Moreover, we found that the expression levels of the related proteins MMP2 and MMP9 increased in MHCC97H-shUSP25 cells overexpressing TRIM21 [Figure 6K]. Finally, our results showed that the Wnt/ $\beta$ -catenin pathway and EMT were activated upon TRIM21 overexpression in MHCC97H-shUSP25 cells [Figure 6K]. In conclusion, these data validate our hypothesis that USP25 interacts with TRIM21 to activate the Wnt/ $\beta$ -catenin signaling pathway to regulate EMT.

### USP25 promotes tumor growth *in vivo*

To verify the role played by USP25 *in vivo*, we constructed a mouse liver cancer model with the USP25 gene deletion. The mice were assigned to four groups: the USP25<sup>-/-</sup>/DEN, WT/DEN, USP25<sup>-/-</sup>/PBS, and WT/PBS groups. After DEN/PBS treatment for 30 weeks, the liver/body weight ratio, number of tumors, and tumor-occupied area were significantly higher in the WT/DEN group than in the USP25<sup>-/-</sup>/DEN group, and in the USP25<sup>-/-</sup>/PBS and WT/PBS groups, very few nodules formed [Figure 7A, B]. Subsequently, compared to the USP25<sup>-/-</sup>/PBS and WT/PBS groups, the HE staining results of liver tissues demonstrated abundant hepatic sinusoids, increased nucleus-to-cytoplasm ratio, and obvious nuclear atypia in the USP25<sup>-/-</sup>/DEN and WT/DEN groups [Figure 7C]. Moreover, the results of reticular fiber staining suggested that the normal radial structure of the hepatic plates was destroyed, the number of hepatic plate layers increased, and the arrangement of tumor cells was disordered in the USP25<sup>-/-</sup>/DEN and WT/DEN groups compared to the corresponding control group [Figure 7D]. To further confirm the effect of

USP25 on distant tumor metastasis, HE staining of lung tissue was preformed and revealed that the normal alveolar structure disappeared in the WT/DEN group, and metastatic nodules containing HCC cells were observed in the lungs [Figure 7E]. Finally, sections of mouse liver tissues were subjected to IHC staining, and the results showed high expression of E-cadherin and low expression of N-cadherin with obviously more intense staining of the cell membrane in the USP25<sup>-/-</sup>/DEN group than in the WT/DEN group, and the expression level of  $\beta$ -catenin was increased in the WT/DEN group [Figure 7F].

### Discussion

HCC, a rapidly progressing malignancy, is the sixth most common cancer and the third leading cause of cancer-related death worldwide; it accounts for approximately 906,000 new cases and 830,000 deaths per year.<sup>[12,13]</sup> Surgical treatment remains the preferred treatment for patients, especially at an early stage.<sup>[14]</sup> However, most patients still have a poor prognosis and low overall survival. To improve clinical outcomes, it is important to find novel therapeutic targets.

The ubiquitin-proteasome system (UPS) is a key regulator that maintains cellular function and stability and is mainly composed of E1 activating enzymes, E2 conjugating enzymes, E3 ubiquitin ligases, the proteasome, and deubiquitinating enzymes.<sup>[15]</sup> The UPS participates in various cellular biological processes, such as the cell cycle, gene transcription, cellular differentiation, and apoptosis, which are important for maintaining the normal physiological functions of cells.<sup>[16]</sup> Based on sequence homology and structural similarity, DUBs are classified into seven subfamilies, and USP25 belongs to the largest ubiquitin-specific protease (USP) subfamily.<sup>[17]</sup> Multiple studies have shown that USP25, an important regulator, can interact with a large number of signaling molecules and participate in the regulation of various intracellular signaling pathways, especially in the development of tumors.<sup>[18]</sup> A recent study verified that USP25 is highly expressed in colon tumors, activates the Wnt signaling pathway, and is involved in the phosphorylation of signaling transcription factor activator 3 (STAT3) to promote colon tumorigenesis.<sup>[19]</sup> Another study reported that high expression of USP25 leads to the accumulation of  $\beta$ -catenin, which activates the Wnt/ $\beta$ -catenin signaling pathway and thus promotes tumor growth and the proliferation and migration of prostate cancer cells.<sup>[20]</sup> Moreover, USP25 has been shown to play a similar role in non-small cell lung cancer and breast cancer.<sup>[21,22]</sup> However, its function and mechanism in HCC have not been investigated. In our study, we first analyzed the expression of USP25 in HCC based on the TCGA and ICGC databases and then showed that USP25 was highly expressed in HCC cell lines. Subsequently, according to a series of experiments, we observed that overexpression of USP25 promoted HCC cell proliferation, migration, and invasion both *in vitro* and *in vivo*; in particular, HCC cells noticeably spread to the lungs. However, further study is warranted to confirm the mechanism of USP25 in HCC.

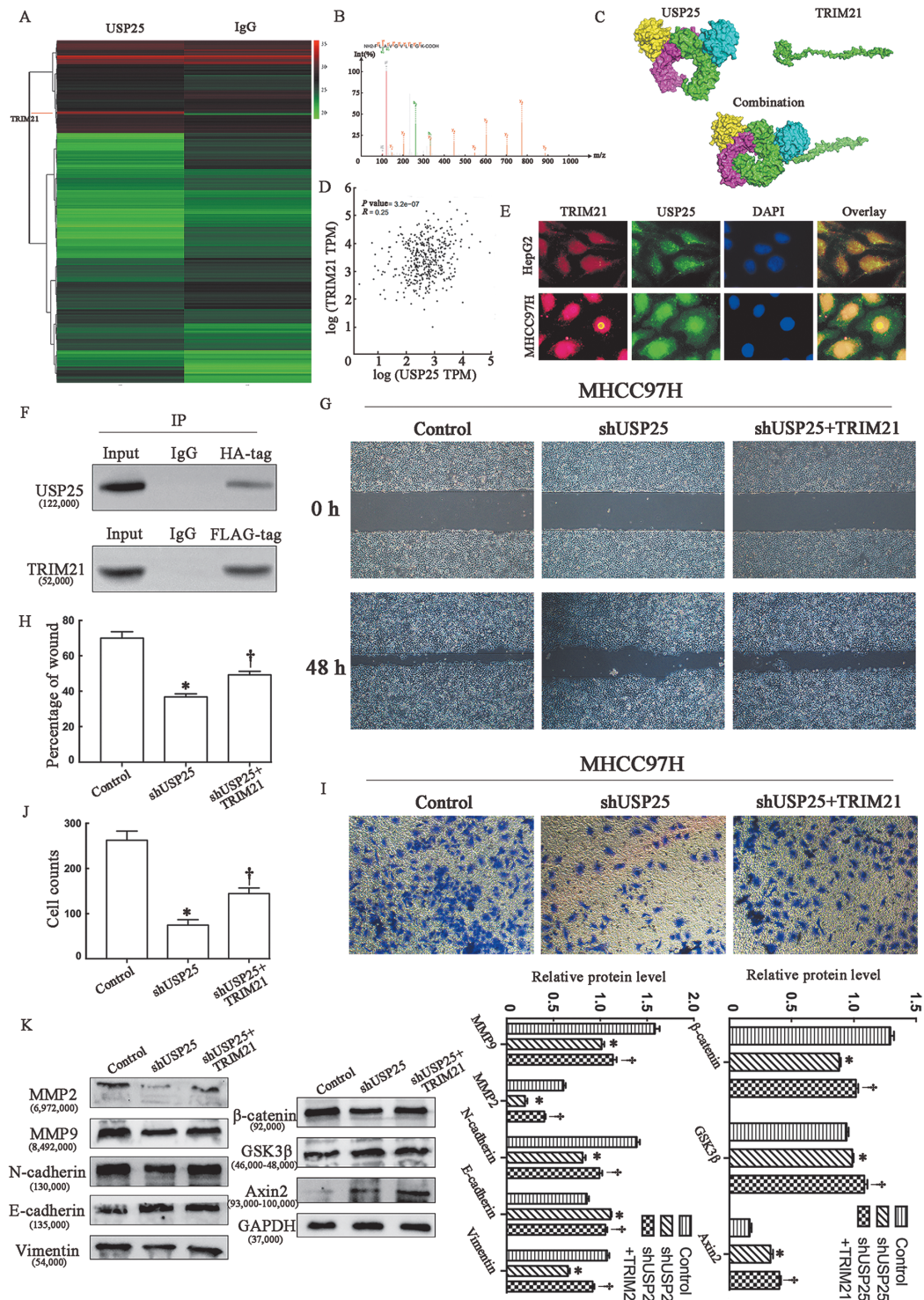


**Figure 6:** USP25 interacts with TRIM21 to activate the Wnt/ $\beta$ -catenin signaling pathway. (A,B) Mass spectrometry indicated a relationship between USP25 and TRIM21. (C) Molecular docking showed the interaction between USP25 and TRIM21. (D) USP25 was positively correlated with TRIM21 in the TCGA database ( $n = 408$ ). (E) IF staining showed that USP25 and TRIM21 were located in both the cytoplasm and nuclei (Original magnification  $\times 200$ ). (F) A Co-IP assay verified a protein–protein interaction between USP25 and TRIM21. (G–J) TRIM21 overexpression in MHCC97H cells rescued the migration and invasion that had been weakened by the USP25 knockdown (G: Original magnification  $\times 40$ , I: Original magnification  $\times 100$ ). (K) The Wnt/ $\beta$ -catenin pathway and EMT were activated by TRIM21 overexpression in MHCC97H-shUSP25 cells. \* $P < 0.05$ , shUSP25 group vs. control group; † $P < 0.05$ , shUSP25+TRIM21 group vs. control group Co-IP; Coimmunoprecipitation; EMT: Epithelial–mesenchymal transition; IF: Immunofluorescence; TRIM21: Tripartite motif-containing 21; USP25: Ubiquitin-specific peptidase 25; DAPI: 4',6-Diamidino-2'-phenylindole; HA: Hemagglutinin; shUSP25: Short hairpin Ubiquitin-specific peptidase 25; MMP2: Matrix metalloproteinase 2; MMP9: Matrix metalloproteinase 9; GAPDH: Glyceraldehyde-3-phosphate dehydrogenase; TCGA: The Cancer Genome Atlas.

The Wnt/ $\beta$ -catenin pathway is an evolutionarily conserved signaling pathway composed of Wnt proteins, Frizzled receptor family members, the casein kinase 1 (CK1) and

dishevelled (Dvl) proteins, the  $\beta$ -catenin/Axin/APC/GSK3 $\beta$  complex and Lymphoid enhancer factor/T cell factor transcription factors.<sup>[23]</sup> When abnormally activated, the

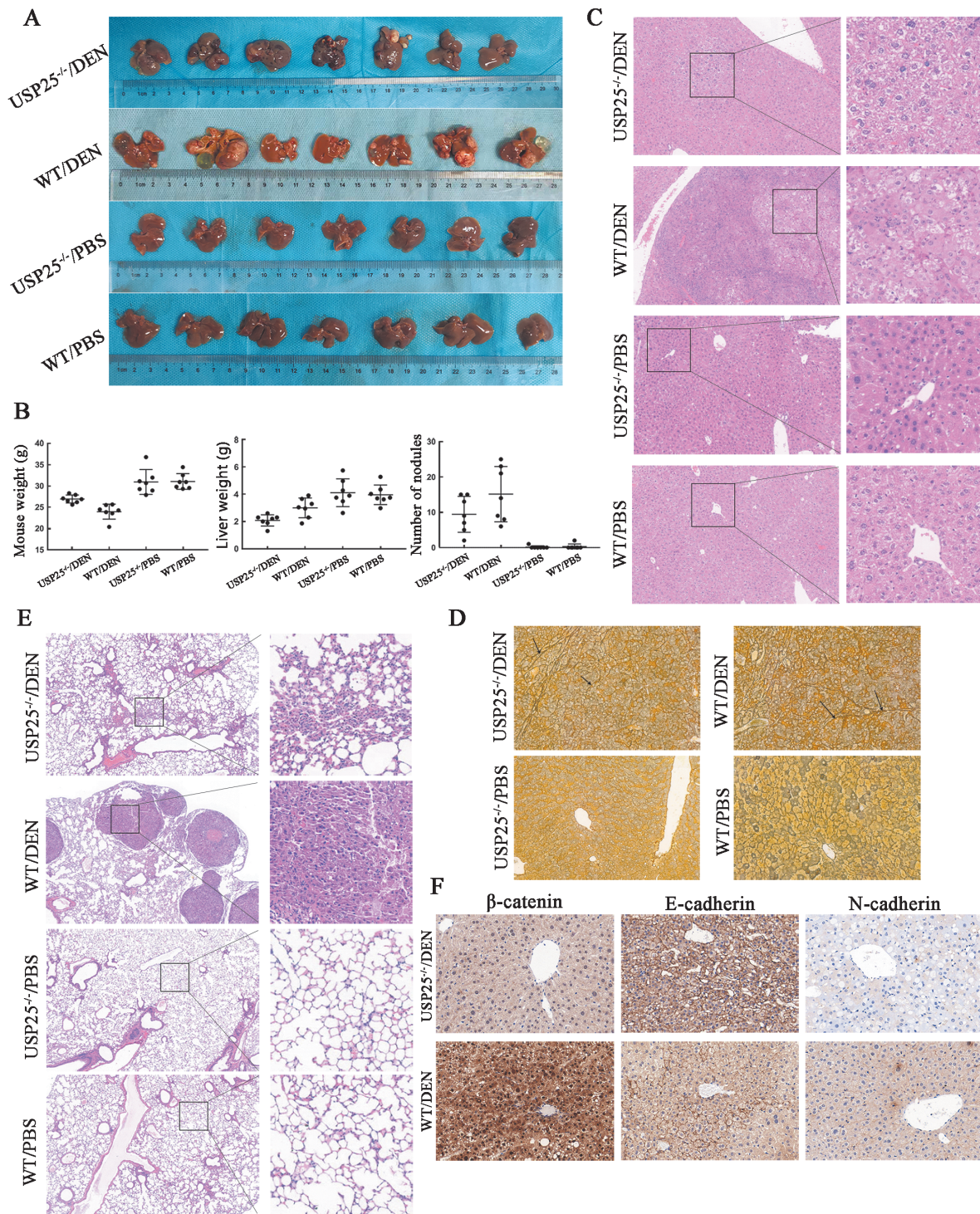


**Figure 7:** USP25 promotes tumor growth *in vivo*. (A) Liver appearance in the mice from each group. (B) Statistical graphs show the mouse weights, liver weights, and the number of nodules. (C) HE staining of the liver tissues (Original magnification  $\times 40$ ). (D) Reticular fiber staining was used to distinguish tumor tissues from normal tissues (Original magnification  $\times 100$ ). (E) HE staining of the lung tissues (Original magnification  $\times 40$ ). (F) IHC assay showed the expression of  $\beta$ -catenin, E-cadherin, and N-cadherin (Original magnification  $\times 140$ ). HE: Hematoxylin and eosin; IHC: Immunohistochemistry; USP25: Ubiquitin-specific peptidase 25; WT: Wild type; DEN: N-diethylnitrosamine; PBS: Phosphate buffered saline

ligand-protein Wnt can bind to the receptor protein Frizzled, which activates Dvl, promoting the dissolution of the complex and causing the large-scale accumulation of  $\beta$ -catenin in the nucleus. Then,  $\beta$ -catenin binds to the intranuclear transcription factor LEF/TCF to affect tumor formation and progression through downstream target genes such as C-myc and Cyclin D1.<sup>[24,25]</sup> EMT

refers to the biological process in which epithelial cells are transformed into cells with a mesenchymal cell phenotype through a specific program. Cadherins are important markers of EMT, and the E-cadherin/ $\beta$ -catenin complex plays an important role in maintaining normal epithelial morphology and cell-cell adhesion.<sup>[26]</sup> When Wnt signaling is activated,  $\beta$ -catenin phosphoryla-

tion influences the stability of the E-cadherin/ $\beta$ -catenin complex, decreasing E-cadherin-mediated adhesion and disrupting the intercellular connection, thereby resulting in the enhanced invasion and migration of tumor cells.<sup>[27]</sup> The role of the Wnt/ $\beta$ -catenin pathway in the progression of HCC has been established.<sup>[28]</sup> For example, several studies have shown the nuclear accumulation of  $\beta$ -catenin in HCC, and the abnormal expression of key genes augments Wnt/ $\beta$ -catenin signaling activity.<sup>[29]</sup> Our research led to similar conclusions: the expression of  $\beta$ -catenin, C-myc, and Cyclin D1 increased, while the expression levels of Axin2, APC, and GSK3 $\beta$  decreased in HCC cell lines overexpressing USP25. Moreover, the EMT-related protein E-cadherin was expressed at a low level, and N-cadherin was highly expressed. After the addition of the signaling pathway inhibitor XAV939, the expression of these proteins was inhibited. In addition, we carried out animal experiments to verify our findings.

To clarify the mechanism of the *USP25* gene, mass spectrometry experiments were performed. We found that interaction with TRIM21 was necessary for the USP25 function. TRIM21, a member of the TRIM family, is expressed in both the cytoplasm and nucleus, and the gene encoding this protein is located on chromosome 11.<sup>[30]</sup> The RING domain at the amino-terminal region of the TRIM21 protein exhibits E3 ubiquitin ligase activity.<sup>[31]</sup> Notably, ultraviolet (UV) irradiation induced apoptosis of human breast cancer cells, and the RNA-binding protein HuR activated the tumor suppressor p53 mRNA translation, while TRIM21 expression induced by UV irradiation mediated the proteasomal degradation of HuR and reduced P53 levels.<sup>[32]</sup> Additionally, during radiotherapy of nasopharyngeal carcinoma (NPC), TRIM21 was shown to inhibit TP53 expression by mediating the ubiquitination and degradation of guanine monophosphate synthase (GMPS), and

overexpression of TRIM21 protected NPC cells from radiation-mediated apoptosis.<sup>[33]</sup> However, Ding *et al*<sup>[34]</sup> found that *TRIM21* knockdown in HCC cell lines significantly enhanced HCC cell proliferation, colony formation, migration, and antiapoptotic activity *in vitro*, but the mechanisms of these functions were not extensively explored. Considering our experimental results, we speculated that TRIM21 recruits more ubiquitin to bind  $\beta$ -catenin, which leads to  $\beta$ -catenin degradation through the ubiquitination pathway, whereas USP25 disrupts the ubiquitination pathway, causing  $\beta$ -catenin accumulation in the nucleus and activating the Wnt/ $\beta$ -catenin signaling pathway. Therefore, USP25 is expected to be a potential therapeutic target for HCC, and it is necessary to develop USP25 inhibitors. The FDA-approved drug vismodegib can treat basal cell carcinoma by inhibiting the Hedgehog (Hh) signaling pathway and has been shown to be an inhibitor of USP25. It can inhibit the expression levels of signaling pathway-associated substrate proteins, such as C-myc, Notch1, and tankyrase-1/2.<sup>[19]</sup> Furthermore, the study found that another group of compounds, AZ1 through AZ4, were able to non-competitively inhibit both USP25 and USP28.<sup>[35]</sup> Accordingly, in a mouse model, AZ1 was found to impair USP25-induced intestinal bacterial infection, enhance the immune response, and inhibit the role of USP25 in promoting the process of intestinal cancer.<sup>[19]</sup> Unfortunately, the development of selective inhibitors of USP25 may be challenging due to the high sequence similarity of USP25 and USP28.

In summary, in the current study, we identified the overexpression of USP25 in HCC cell lines for the first time. The results from these assays indicated that USP25 promotes HCC cell proliferation, migration, and invasion by interacting with TRIM21, thereby regulating the Wnt/ $\beta$ -catenin signaling pathway and EMT [Figure 8].

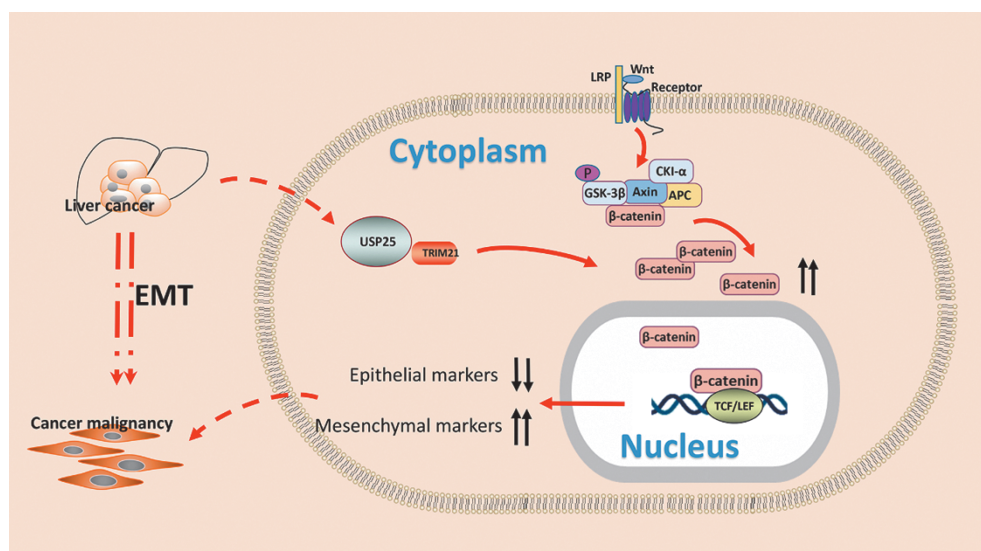


**Figure 8:** USP25 promotes HCC progression by interacting with TRIM21 via the Wnt/ $\beta$ -catenin signaling pathway. HCC: Hepatocellular carcinoma; TRIM21: Tripartite motif-containing 21; USP25: Ubiquitin-specific peptidase 25; EMT: Epithelial–mesenchymal transition; TCF: T cell factor; LEF: Lymphoid enhancer factor; LRP: Lipoprotein receptor-related protein; APC: Adenomatous polyposis coli; GSK3 $\beta$ :Glycogen synthase kinase 3 beta.

## Funding

This study was supported by the National Natural Science Foundation of China (No. 81870392).

## Conflicts of interest

None.

## References

- Craig AJ, von Felden J, Garcia-Lezana T, Sarcognato S, Villanueva A. Tumour evolution in hepatocellular carcinoma. *Nat Rev Gastroenterol Hepatol* 2020;17:139–152. doi: 10.1038/s41575-019-0229-4.
- Cao W, Chen HD, Yu YW, Li N, Chen WQ. Changing profiles of cancer burden worldwide and in China: a secondary analysis of the global cancer statistics 2020. *Chin Med J* 2021;134:783–791. doi: 10.1097/CM9.0000000000001474.
- Thandra KC, Barsouk A, Saginala K, Aluru JS, Rawla P, Barsouk A. Epidemiology of non-alcoholic fatty liver disease and risk of hepatocellular carcinoma progression. *Clin Exp Hepatol* 2020;6:289–294. doi: 10.5114/ceh.2020.102153.
- Kim SY, Baek KH. TGF- $\beta$  signaling pathway mediated by deubiquitinating enzymes. *Cell Mol Life Sci* 2019;76:653–665. doi: 10.1007/s00018-018-2949-y.
- He M, Zhou Z, Wu G, Chen Q, Wan Y. Emerging role of DUBs in tumor metastasis and apoptosis: Therapeutic implication. *Pharmacol Ther* 2017;177:96–107. doi: 10.1016/j.pharmthera.2017.03.001.
- Kee Y, Huang TT. Role of deubiquitinating enzymes in DNA repair. *Mol Cell Biol* 2015;36:524–544. doi: 10.1128/MCB.00847-15.
- Zhong B, Liu X, Wang X, Chang SH, Liu X, Wang A, *et al.* Negative regulation of IL-17-mediated signaling and inflammation by the ubiquitin-specific protease USP25. *Nat Immunol* 2012;13:1110–1117. doi: 10.1038/ni.2427.
- Zhu W, Zheng D, Wang D, Yang L, Zhao C, Huang X. Emerging roles of ubiquitin-specific protease 25 in diseases. *Front Cell Dev Biol* 2021;9:698751. doi: 10.3389/fcell.2021.698751.
- Xu D, Liu J, Fu T, Shan B, Qian L, Pan L, *et al.* USP25 regulates Wnt signaling by controlling the stability of tankyrases. *Genes Dev* 2017;31:1024–1035. doi: 10.1101/gad.300889.117.
- Niehrs C. The complex world of WNT receptor signalling. *Nat Rev Mol Cell Biol* 2012;13:767–779. doi: 10.1038/nrm3470.
- Liu J, Xiao Q, Xiao J, Niu C, Li Y, Zhang X, *et al.* Wnt/ $\beta$ -catenin signalling: Function, biological mechanisms, and therapeutic opportunities. *Signal Transduct Target Ther* 2022;7:3. doi: 10.1038/s41392-021-00762-6.
- Xia C, Dong X, Li H, Cao M, Sun D, He S, *et al.* Cancer statistics in China and United States, 2022: Profiles, trends, and determinants. *Chin Med J* 2022;135:584–590. doi: 10.1097/CM9.0000000000002108.
- Sung H, Ferlay J, Siegel RL, Laversanne M, Soerjomataram I, Jemal A, *et al.* Global cancer statistics 2020: GLOBOCAN estimates of incidence and mortality worldwide for 36 cancers in 185 countries. *CA Cancer J Clin* 2021;71:209–249. doi: 10.3322/caac.21660.
- Kanwal F, Singal AG. Surveillance for hepatocellular carcinoma: Current best practice and future direction. *Gastroenterology* 2019;157:54–64. doi: 10.1053/j.gastro.2019.02.049.
- Engel K, Bassermann F. The ubiquitin proteasome system and its implications for oncology (in German). *Dtsch Med Wochenschr* 2013;138:1178–82. doi: 10.1055/s-0033-1343110.
- Thompson SJ, Loftus LT, Ashley MD, Meller R. Ubiquitin-proteasome system as a modulator of cell fate. *Curr Opin Pharmacol* 2008;8:90–95. doi: 10.1016/j.coph.2007.09.010.
- Wang Y, Wang F. Post-translational modifications of deubiquitinating enzymes: Expanding the ubiquitin code. *Front Pharmacol* 2021;12:685011. doi: 10.3389/fphar.2021.685011.
- Sauer F, Klemm T, Kollampally RB, Tessmer I, Nair RK, Popov N, *et al.* Differential oligomerization of the deubiquitinases USP25 and USP28 regulates their activities. *Mol Cell* 2019;74:421–435. e10. doi: 10.1016/j.molcel.2019.02.029.
- Wang XM, Yang C, Zhao Y, Xu ZG, Yang W, Wang P, *et al.* The deubiquitinase USP25 supports colonic inflammation and bacterial infection and promotes colorectal cancer. *Nat Cancer* 2020;1:811–825. doi: 10.1038/s43018-020-0089-4.
- Cheng H, Li X, Wang C, Chen Y, Li S, Tan J, *et al.* Inhibition of tankyrase by a novel small molecule significantly attenuates prostate cancer cell proliferation. *Cancer Lett* 2019;443:80–90. doi: 10.1016/j.canlet.2018.11.013.
- Li J, Tan Q, Yan M, Liu L, Lin H, Zhao F, *et al.* miRNA-200c inhibits invasion and metastasis of human non-small cell lung cancer by directly targeting ubiquitin specific peptidase 25. *Mol Cancer* 2014;13:166. doi: 10.1186/1476-4598-13-166.
- Deng S, Zhou H, Xiong R, Lu Y, Yan D, Xing T, *et al.* Over-expression of genes and proteins of ubiquitin specific peptidases (USPs) and proteasome subunits (PSs) in breast cancer tissue observed by the methods of RFDD-PCR and proteomics. *Breast Cancer Res Treat* 2007;104:21–30. doi: 10.1007/s10549-006-9393-7.
- Van Kappel EC, Maurice MM. Molecular regulation and pharmacological targeting of the  $\beta$ -catenin destruction complex. *Br J Pharmacol* 2017;174:4575–4588. doi: 10.1111/bph.13922.
- Masuda T, Ishitani T. Context-dependent regulation of the  $\beta$ -catenin transcriptional complex supports diverse functions of Wnt/ $\beta$ -catenin signaling. *J Biochem* 2017;161:9–17. doi: 10.1093/jb/mvw072.
- Taciak B, Pruszyńska I, Kiraga L, Bialasek M, Krol M. Wnt signaling pathway in development and cancer. *J Physiol Pharmacol* 2018;69. doi: 10.26402/jpp.2018.2.07.
- Wijnhoven BP, Dinjens WN, Pignatelli M. E-cadherin-catenin cell-cell adhesion complex and human cancer. *Br J Surg* 2000;87:992–1005. doi: 10.1046/j.1365-2168.2000.01513.x.
- Ilyas M, Tomlinson IP. The interactions of APC, E-cadherin and beta-catenin in tumour development and progression. *J Pathol* 1997;182:128–137. doi: 10.1002/(SICI)1096-9896(199706)182:2<128::AID-PATH839>3.0.CO;2-Q.
- Wang W, Smits R, Hao H, He C. Wnt/ $\beta$ -catenin signaling in liver cancers. *Cancers (Basel)* 2019;11:926. doi: 10.3390/cancers11070926.
- Monga SP.  $\beta$ -catenin signaling and roles in liver homeostasis, injury, and tumorigenesis. *Gastroenterology* 2015;148:1294–1310. doi: 10.1053/j.gastro.2015.02.056.
- Frank MB, Itoh K, Fujisaku A, Pontarotti P, Mattei MG, Neas BR. The mapping of the human 52-kD Ro/SSA autoantigen gene to human chromosome 11, and its polymorphisms. *Am J Hum Genet* 1993;52:183–191.
- Meroni G, Diez-Roux G. TRIM/RBCC, a novel class of ‘single protein RING finger’ E3 ubiquitin ligases. *Bioessays* 2005;27:1147–1157. doi: 10.1002/bies.20304.
- Guha A, Ahuja D, Das Mandal S, Parasar B, Deyasi K, Roy D, *et al.* Integrated regulation of HuR by translation repression and protein degradation determines pulsatile expression of p53 under DNA damage. *iScience* 2019;15:342–359. doi: 10.1016/j.isci.2019.05.002.
- Zhang P, Li X, He Q, Zhang L, Song K, Yang X, *et al.* TRIM21-SERPINB5 aids GMPs repression to protect nasopharyngeal carcinoma cells from radiation-induced apoptosis. *J Biomed Sci* 2020;27:30. doi: 10.1186/s12929-020-0625-7.
- Ding Q, He D, He K, Zhang Q, Tang M, Dai J, *et al.* Downregulation of TRIM21 contributes to hepatocellular carcinoma carcinogenesis and indicates poor prognosis of cancers. *Tumour Biol* 2015;36:8761–8772. doi: 10.1007/s13277-015-3572-2.
- Wrigley JD, Gavory G, Simpson I, Preston M, Plant H, Bradley J, *et al.* Identification and characterization of dual inhibitors of the USP25/28 deubiquitinating enzyme subfamily. *ACS Chem Biol* 2017;12:3113–3125. doi: 10.1021/acscmbio.7b00334.

**How to cite this article:** Liu YH, Ma JJ, Lu SM, He PZ, Dong WG. USP25 promotes hepatocellular carcinoma progression by interacting with TRIM21 via the Wnt/ $\beta$ -catenin signaling pathway. *Chin Med J* 2023;136:2229–2242. doi: 10.1097/CM9.0000000000002714